Chemical Engineering Journal 165 (2010) 301–309

Contents lists available at ScienceDirect

Chemical Engineering Journal

journal homepage: www.elsevier.com/locate/cej

A study on the synergistic adsorptive and photocatalytic activities of $TiO_{2-x}N_x$/Beta composite catalysts under visible light irradiation

Qun Shen [a,b], Wei Zhang [a], Zhengping Hao [b], Linda Zou [a,*]

[a] Centre for Water Management and Reuse, University of South Australia, Mawson Lakes, South Australia, 5095, Australia
[b] Department of Environmental Nano-materials, Research Center for Eco-Environmental Sciences, Chinese Academy of Sciences, Beijing 100085, PR China

ARTICLE INFO

Article history:
Received 19 January 2010
Received in revised form 19 August 2010
Accepted 24 August 2010

Keywords:
Nitrogen-doped titania
Beta zeolite
Composite
Photodegradation
Visible light irradiation

ABSTRACT

A series of $TiO_{2-x}N_x$/Beta composite samples were prepared by coating the nitrogen-doped titania on the Beta zeolite using a simple sol–gel method. Samples were characterized by nitrogen adsorption–desorption, XRD, TEM, UV–vis, XPS and FTIR techniques. The photocatalytic activities were evaluated by the degradation of methylene blue under visible light irradiation. The synergistic effect between absorption and photocatalysis of the $TiO_{2-x}N_x$/Beta composite materials was found in terms of methylene blue removal efficiency under visible light irradiation, since the assisting adsorption ability from H-Beta zeolite could supply a concentrated pollutant environment around titania active sites. The highest photocatalytic efficiency was obtained on the 10% $TiO_{2-x}N_x$-coated composite sample, which was probably due to the better dispersion of titania on the support. Furthermore, the $TiO_{2-x}N_x$/Beta-10% catalyst was consistent to be the most efficient composite material tested for the photocatalytic degradation of methylene blue even in different pH environment.

1. Introduction

In recent years, industrialization and agricultural development, together with rapid urbanisation, have caused ever increasing pollution especially on water resources. Various kinds of contaminants enter into our water sources, most of them through industrial wastewater discharge. Developing effective wastewater treatment technologies is a challenging task to most researchers [1,2]. Recently, extensive efforts have been made to investigate the use of photocatalysis for the destruction and removal of highly toxic organic compounds in wastewater purification. Titanium oxides as photocatalysts have attracted a great deal of attention, due to its high photocatalytic activity, resistance to photocorrosion, photostability, low cost and non-toxicity [3]. It is generally accepted that fine nano-sized TiO_2 particles are favourable for attaining higher photoactivity compared to bulky large particles. Therefore, many attempts have been made to prepare the photocatalyst with finer particle size and narrower size distribution. However, in practical applications, dispersing photocatalysts in the form of fine particles in water is difficult, and such is separation or recovery [4]. On the other hand, pollutants in the wastewater often exist in low concentration (order of ppm or below) and the low concentration contaminants near TiO_2 catalyst is not favourable for surface contact-based photocatalytic reaction [5]. In order to achieve rapid and efficient decomposition of organic pollutants and put it to the practical use, great efforts have been made to design composite materials of TiO_2 powder immobilized on inert and suitable porous materials, such as mesoporous silica [6–9], activated carbon [10–13] and zeolite [14–21]. Among many porous materials, zeolites exhibit several specific features, which make them suitable for being used as host candidates for photocatalysts. These are (i) more photochemical stability and thermal and chemical inertness; (ii) reasonable transparency to UV–vis radiations above 240 nm allowing light of certain wavelength to reach the catalysts and pollutants at intraparticle positions; (iii) high adsorptive capacity for concentrating the organic compounds from solution to the active sites of the photocatalysts on the substrate; (iv) the ability of the zeolite framework to participate actively in the electron-transfer process, either as an electron acceptor or an electron donor [22]. However, so far most of the composite materials reported in the literatures were only photocatalytically active under UV light irradiation [23]. It is well known in the overall solar radiation reaching the earth's surface, ultraviolet light only contribute to <5% [24]. Therefore, this with no doubt would restrict the practical application of these kinds of composite materials in future use.

Recently researchers found that pure TiO_2 modified by metal [25,26] and non-metal doping processes [3,24,27–33] could lead to visible light photocatalysis. However, metal doping has several drawbacks, such as thermal instability and high cost. Therefore, anionic dopant seems to be more attractive than metal ions at

* Corresponding author. Tel.: +61 8 8302 5489; fax: +61 8 8302 3386.
E-mail address: linda.zou@unisa.edu.au (L. Zou).

1385-8947/$ – see front matter © 2010 Elsevier B.V. All rights reserved.
doi:10.1016/j.cej.2010.08.057

Table 1
The physicochemical properties of the bare $TiO_{2-x}N_x$ and the composite samples.

Samples	Titanium crystallite size from XRD (nm)	S_{BET} ($m^2\ g^{-1}$)	1st $E_{band\ gap}$ (eV)	2nd $E_{band\ gap}$ (eV)
H-Beta	–	523.6	–	–
$TiO_{2-x}N_x$/Beta-10%	–	315.6	3.28	2.66
$TiO_{2-x}N_x$/Beta-40%	5	274.8	3.28	2.40
$TiO_{2-x}N_x$/Beta-90%	5	228.3	3.28	2.53
Bare $TiO_{2-x}N_x$	5	272.1	3.26	2.57

the moment. Furthermore, latest efforts on calculated densities of states (DOSs) of the doped anion in the anatase TiO_2 crystal revealed that nitrogen doping could be the most effective choice for inducing photocatalytic activity under visible light irradiation, which was also confirmed by several experiment results [5,28,33]. To the best of our knowledge, only few literatures about titania/adsorbent composite photocatalysts via sol–gel nitrogen doping preparation are reported [34–36], which certainly deserve more research attention. Therefore, in this article we developed a series of $TiO_{2-x}N_x$/Beta composite photocatalyst with different titania loading. The obtained composite photocatalysts were characterized by nitrogen adsorption–desorption, XRD, UV–vis reflectance, XPS, FTIR and TEM. In addition, we studied the photocatalytic activities of the $TiO_{2-x}N_x$/Beta composite under visible light irradiation by using methylene blue as a model pollutant. The influence of H-Beta zeolite involvement as porous support on the structure and photocatalytic activities of N-doped TiO_2 nanoparticles was also discussed.

2. Experimental and methods

2.1. Materials and chemicals

Commercial Beta zeolite (Si/Al = 10.8) was purchased from Sinopec Co (Tianjin, China) and it was calcined at 500 °C for 4 h before being used in the sample preparation. The chemicals used for the synthesis were titanium butoxides ($Ti(OC_4H_9)_4$, 97%, Aldrich), HCl (65.5%, BDH Chemicals, Australia), ethanol (100%, Scharlau). Methylene blue was obtained from Sigma-Aldrich. All the chemicals were used as supplied without further purification. Deionized water, purified with a water purification system (Diamond, Barnstead), was used for preparing solutions in the experiments.

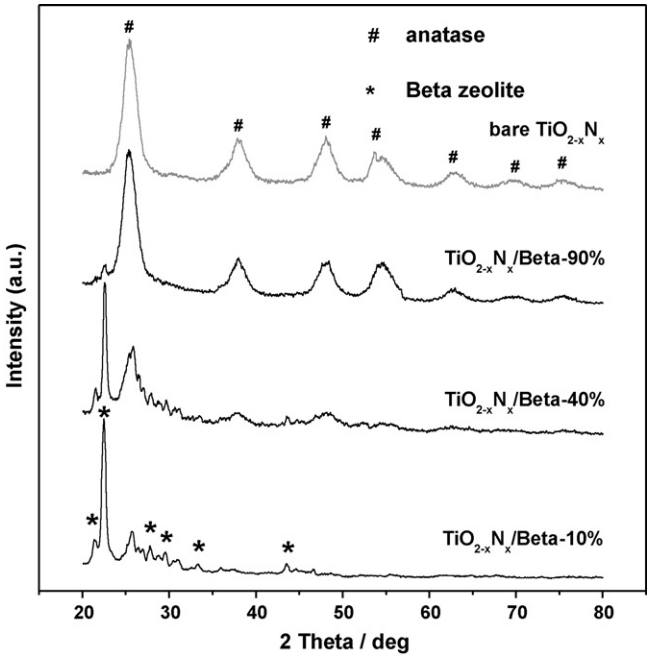

Fig. 1. XRD patterns of the naked $TiO_{2-x}N_x$ and $TiO_{2-x}N_x$/Beta-*x*% composites samples coated with 10%, 40% and 90% titania loading.

2.2. Preparation of TiO_2-N/Beta composite catalysts

The TiO_2 nanoparticles were synthesized by hydrolysis of precursor chemicals to form a transparent sol using the following method: 50 ml of titanium butoxide ($Ti(OC_4H_9)_4$, 97%) was dissolved in ethanol (200 ml). The solution was stirred for 30 min at room temperature followed by addition of a mixture of deionized water and nitric acid under vigorous stirring. The solution was then successively stirred at room temperature till a clear transparent sol was obtained. To introduce the nitrogen dopant into the titanium nanoparticles, triethylamine (N/Ti = 1.0) was added drop-wise into the above titanium solution. Sol was formed immediately and vigorously stirred for another 10 h. Depending on the (wt.%) loading of TiO_2 on the catalyst, certain amount of H-Beta zeolite was added to the titanium sol. The resulting mixed suspension was continuously stirred for 5 h. Finally, the resulting N-doped titania zeolite catalyst samples were dried at 105 °C for 10 h and calcined in an air atmosphere at 350 °C with temperature ramping at 5 °C min^{-1} and maintained for 2 h. The synthesized samples were denoted as $TiO_{2-x}N_x$/Beta-*x*%, where *x* is the titania content. The bare $TiO_{2-x}N_x$ sample without the addition of Beta zeolite, were also prepared under the same experimental conditions as a reference.

2.3. Catalysts characterization

The specific surface area of all the composite catalytsts and the bare $TiO_{2-x}N_x$ sample was determined from nitrogen adsorption–desorption isotherms at 77 K using volumetric adsorption equipment (BELSORP mini). The surface area was determined using the BET equation. X-ray powder diffraction (XRD) patterns of all samples were collected in the range 20–80° at ambient temperature using a Mini Material Analyser (Cu Kα radiation, λ = 1.54065 Å), operated at 1 kV and 35 mA. The scan speed was 0.5° min^{-1}. The crystallite size was estimated by using the Scherrer equation:

$$D = \frac{K\lambda}{B\cos\theta} \quad (1)$$

where *B* is the full-width at half-maximum (FWHM) of the diffraction peak, $K = 0.89$ is a coefficient, θ is the diffraction angle, and λ is the X-ray wavelength corresponding to the Cu Kα irradiation. Optical properties of the $TiO_{2-x}N_x$/Beta composite samples were studied by a Cary 100 UV–vis spectrometer in diffuse reflectance mode over the spectral range of 200–800 nm. Surface analysis of the composite materials and the bare N-doped TiO_2 catalysts was carried out by using X-ray photoelectron spectroscopy (XPS). The instrument employed for XPS studies was a SPECS SAGE spectrometer with a Phoibos 150 hemi-spherical analyser, and an MCD-9 detector. The radiation source used was Mg Kα, and was run at 10 kV and 20 mA (200 W). Samples were placed on carbon tape and then inserted directly to the sample stage. Fourier transform infrared (FTIR) spectra were recorded with KBr disks containing the powder sample with the FTIR spectrometer (Shimadzu FTIR 84005). Transmission electron microscopy (TEM) analysis was conducted

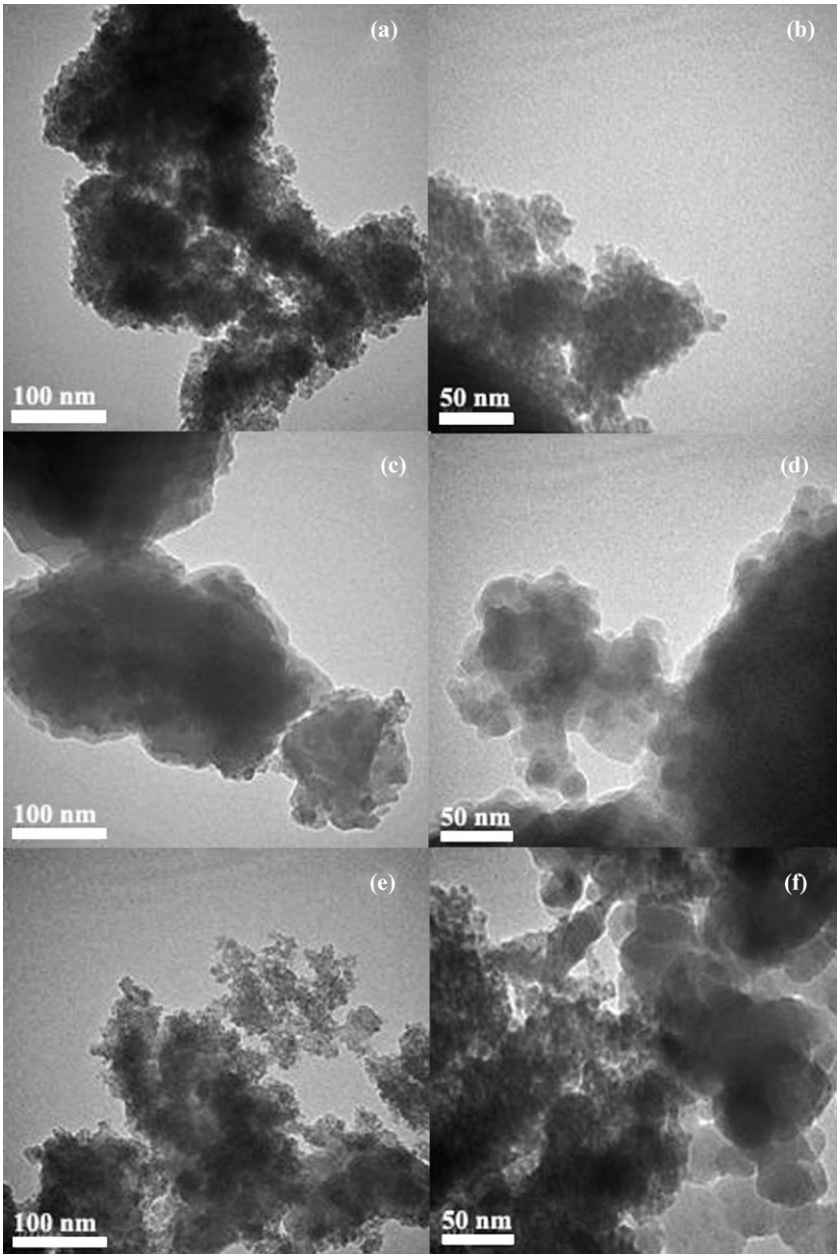

Fig. 2. TEM images of the bare N-doped TiO_2 (a and b), $TiO_{2-x}N_x$/Beta-10% (c and d) and $TiO_{2-x}N_x$/Beta-90% (e and f) samples.

using H-7500 microscopy operating with an acceleration voltage of 80 kV. The samples were prepared by ultrasonication in ethanol, and then evaporating a drop of the resultant suspension onto a carbon support grid.

2.4. Photocatalytic activity test

The photocatalytic activities of $TiO_{2-x}N_x$/Beta composite catalysts were evaluated by measuring the concentration decrease of methylene blue dye (MB) in the solution under visible light irradiation. In order to eliminate the influence of adsorption, prior to the illumination, a suspension containing the catalyst (30 mg) and 100 ml of aqueous solution with 15 ppm of MB was stirred continuously for 2 h in the dark in order to establish the adsorption/desorption equilibrium. Thereafter, the photocatalytic reaction proceeded under visible light irradiation, during which an 80-W Xe lamp equipped with a UV cut-off filter ($\lambda > 460$ nm) was used as a visible light source. At the given time intervals, a *ca.* 2 ml of sample was withdrawn by a syringe from the suspension. The catalyst was separated by centrifugation from the aqueous solution prior to the analysis. The concentration of MB was determined by a Cary 100 UV–vis spectrometer at 650 nm wavelength. For the photocatalytic degradation at different pH value solutions, the pH was adjusted using either NaOH or HNO_3 solution.

3. Results and discussion

3.1. Characterization

The specific surface areas of all samples are listed in Table 1. Compared to the parent H-Beta zeolite, 10% titania coated on the zeolite lead to a great decrease on the BET specific surface area. A higher loading of titania would result in a further decease. However, this tendency alleviated when titania loading increased to 40%

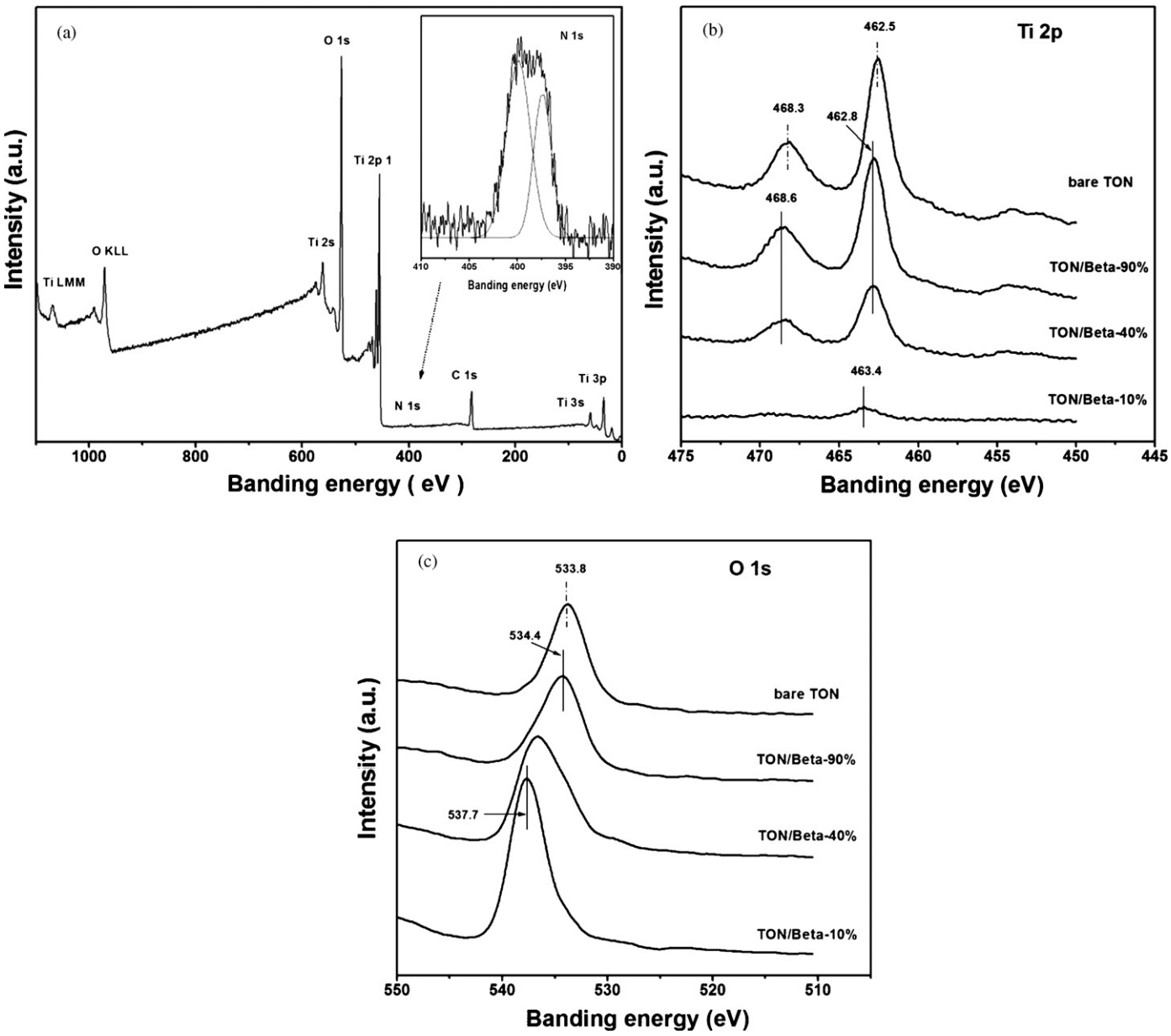

Fig. 3. (a) XPS spectra of the bare N-doped TiO_2 sample in the whole banding energy region and the banding energy region for N1s; The Ti2p region (b) and O1s region (c) of XPS spectra from different samples: the bare N-doped TiO_2 and $TiO_{2-x}N_x$/Beta-*x*% composites samples with different titania loadings.

and 90%. As for the $TiO_{2-x}N_x$/Beta-90% catalyst, the surface area was even smaller than that of the bare N-doped TiO_2 sample. The decreasing trend on the specific surface area indicated that the zeolite support and naked N-doped TiO_2 was not simply a mechanical mixing. Instead, N-doped TiO_2 nanoparticles were dispersed on or inside the support and blocked the zeolite's pore channels partially, which may lead to the apparent decrease of the BET specific surface area.

The XRD patterns of $TiO_{2-x}N_x$/Beta-*x*% catalysts with 10%, 40%, 90% titania loading and the bare $TiO_{2-x}N_x$ sample are displayed in Fig. 1. For the bare N-doped TiO_2 sample the diffraction peaks were all assigned to the anatase crystalline phase, and no other crystal phase (rutile or brookite) was detected. As for the $TiO_{2-x}N_x$/Beta-*x*% catalysts with 40%, 90% titania loadings, besides the anatase crystalline phase, the diffraction peaks assigned to the Beta zeolite were clearly observed. This proves that the zeolite structure was well preserved in the preparation process. For the $TiO_{2-x}N_x$/Beta-10% sample, except the diffraction peaks of zeolite support, no obvious anatase peaks could be seen. This may imply that the titania nanoparticles may be small enough and evenly dispersed on Beta zeolite support. The average crystalline sizes of the photocatalysts were determined according to Scherrer's equation and the results are listed in Table 1. The average crystalline sizes were estimated to be 5 nm for the $TiO_{2-x}N_x$/Beta-*x*% catalysts with 40%, 90% titanium loadings, which was close to that of the bare N-doped TiO_2 sample.

The TEM images of the bare N-doped TiO_2, $TiO_{2-x}N_x$/Beta-10% and $TiO_{2-x}N_x$/Beta-90% samples are shown in Fig. 2. From Fig. 2(a and b), it seems that for the bare TiO_2 sample, the size of TiO_2 nanoparticles is *ca.* 5 nm, which is in good accordance with the XRD calculation. However, the particle aggregation was so severe that massive bulk of titania can be seen in the image. For the image of $TiO_{2-x}N_x$/Beta-10% sample in Fig. 2(c and d), it indicates that the titania particles were in small size and well dispersed on the support. While for the $TiO_{2-x}N_x$/Beta-90% sample in Fig. 6(e and f), except a small part of the titania particles spread on the zeolite surface, most of them are aggregated like the bare N-doped TiO_2.

From the TEM results, it can be conclude that 10% titania loading was suitable to obtain a good dispersion on the zeolite support.

X-ray photoelectron spectroscopy (XPS) was carried out for the surface characterization of the bare N-doped TiO_2 and the $TiO_{2-x}N_x$/Beta composite samples. In Fig. 3(a), it can be seen that a tiny peak is present in the N1s spectra region of the bare N-doped TiO_2 sample and enlarged in the insert of Fig. 3(a). With a suitable spectral deconvolution the peak could be separated into two peaks at *ca.* 400 and 397 eV. It is well known that precise identification of nitrogen species with the banding energy at *ca.* 400 eV is still a challenging topic in the field of nitrogen-doped material, but it is generally accepted that the peak at *ca.* 400 eV may be attribute to the presence of the N atom from adsorbed nitrogen containing compounds on the surface of the samples. As for the peaks in the region of 396–398 eV, they probably arose from O–Ti–N linkages when N atoms replaced the oxygen in the TiO_2 crystal lattice [32,37,38]. Therefore, it is believed that during the sol–gel preparation some nitrogen has been successfully incorporated into the titania lattice and substituted oxygen in the bare N-doped TiO_2 sample.

Fig. 3(b) shows the Ti2p region of the XPS spectra collected from the composite samples with different Ti loading. The bare N-doped TiO_2 acts as a reference sample. The binding energy (BE) of the $Ti2p^{3/2}$ and $Ti2p^{1/2}$ for the bare N-doped TiO_2 sample appear at 462.5 and 468.3 eV. While for the $TiO_{2-x}N_x$/Beta-90% and $TiO_{2-x}N_x$/Beta-40% samples, the Ti2p peak is shifted to the higher banding energy region, which is about 462.8 and 468.6 eV, respectively. Furthermore, more obvious shift can be observed for the $TiO_{2-x}N_x$/Beta-10% sample, for which the $2p^{3/2}$ peak is at *ca.* 463.4 eV and no peak for $Ti2p^{1/2}$ can be clearly found. This result was similar to that observed by Petkowicz et al. [18,39]. Petkowicz et al. think that the shift was caused by the bonding configuration existing between TiO_2 and zeolite, with Ti–O–Si and Ti–O–Al bonds acting as bridges between two materials. In other words, chemical links were thought to exist between TiO_2 and Beta zeolite. From the TEM image in Fig. 2, it can be see that in the $TiO_{2-x}N_x$/Beta-10% sample titania particles were not tend to aggregate but to evenly dispersed on the support. Therefore, it is believed that the chemical link between TiO_2 and Beta zeolite were more pronounced in the $TiO_{2-x}N_x$/Beta-10% sample, which contributed the apparent shift to higher banding energy region in the Ti2p peaks. Further investigation was conducted on the O1s region of XPS spectra for the same samples which are shown in Fig. 3(c). It is believed that for the composite samples, the O1s signals come from two main contributions: first signal around 533.8 eV, related to the O in the formation of nitrogen-doped TiO_2 anatase and second signal at higher banding energy region, related to the O bonded to Si and Al in the zeolite moiety [18]. From Fig. 3(c), it seems that for the composite samples, the peaks of O1s are all moved to the high banding energy region, compared to the N-doped TiO_2 sample, especially for the $TiO_{2-x}N_x$/Beta-10% sample. It means that for all the composite samples, the O1s signal from the zeolite structure made contributions to the overall O1s peak more or less. Petkowicz et al. [18] found that no signal of O1s from the zeolite support could be detected if the layer of Ti completely covers the zeolite surface in the composite samples. Therefore, it can be inferred that in our composite samples, the surface of zeolite was not covered by the Ti compound completely, even when the Ti loading was 90%.

Fig. 4 shows the results of diffuse reflectance spectroscopy. For the parent Beta zeolite, only a very weak absorbance in the ultraviolet region could be observed. As for the $TiO_{2-x}N_x$/Beta-*x*% composite samples, the absorbance behaviour is much different. Strong absorbance was observed and the optical response clearly extended into the visible region, which was similar to the bare N-doped TiO_2 sample. This was resulted from the narrowed band gap after nitrogen incorporation, which also confirmed that the nitrogen incorporation also existed in the titania matrix after coating on

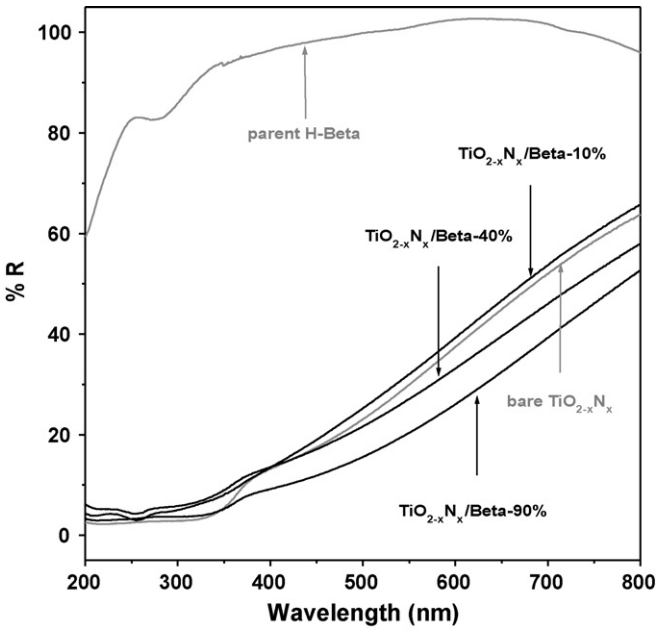

Fig. 4. UV–vis diffuse reflectance spectra of the naked $TiO_{2-x}N_x$ and the $TiO_{2-x}N_x$/Beta-*x*% composite samples with different titania loading.

the Beta support. Furthermore, with TiO_2 loading increasing, further extension occurred. Two absorbance edges located at 370–380 and 460–520 nm appeared, respectively. The appearance of the second absorption edge indicates that a new energy band was formed. The band gap energies are summarized in Table 1.

Fig. 5 shows the FTIR spectra of the $TiO_{2-x}N_x$/Beta-90%, $TiO_{2-x}N_x$/Beta-40%, $TiO_{2-x}N_x$/Beta-10%, and H-Beta samples. The broad peak centred at 3427 cm^{-1} was assigned to the O–H stretching region, and the peak at 1631 cm^{-1} corresponding to the O–H bending vibration of adsorbed water molecules [40]. The peaks in the region of 1250–950, 790–650 and 500–420 cm^{-1} were attributed to the asymmetrical stretching, symmetrical stretching and to (O–Si–O or O–Al–O) deformation, respectively [18]. Sun et al. reported a peak appearing at 934 cm^{-1} after titania was loaded on the SiO_2 support. This was related to the vibration involving a SiO_2 tetrahedron bonded to a titanium atom through Ti–O–Si bonds [39]. The same peak was also observed in our composite samples, espe-

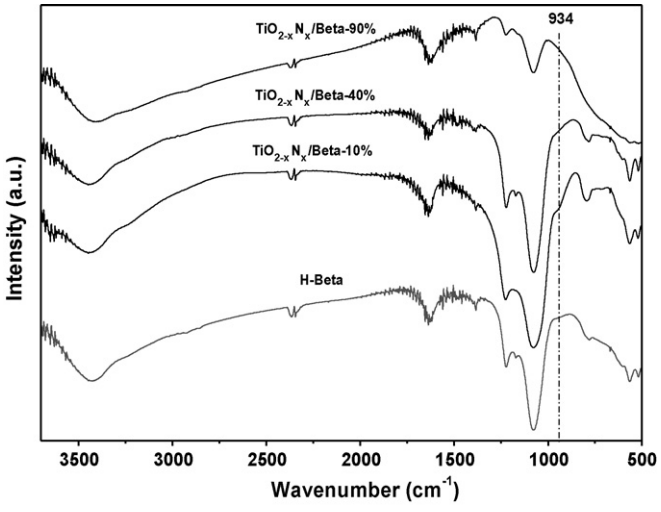

Fig. 5. FTIR spectra of the materials: $TiO_{2-x}N_x$/Beta-90%, $TiO_{2-x}N_x$/Beta-40%, $TiO_{2-x}N_x$/Beta-10%, H-Beta samples.

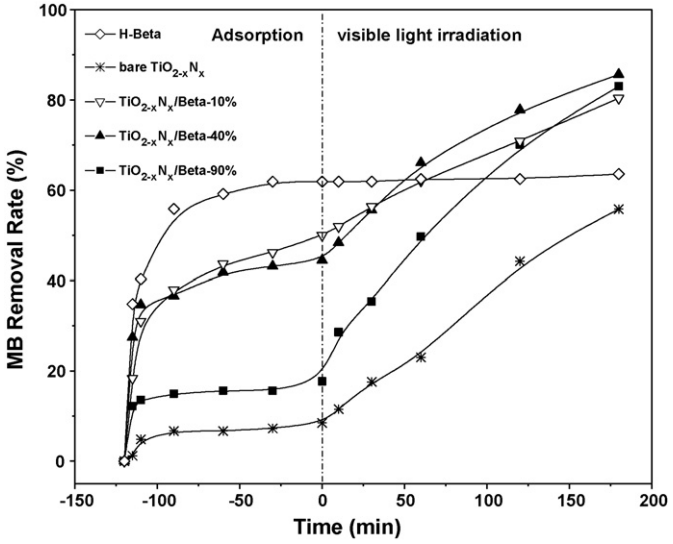

Fig. 6. Removal efficiency of MB on $TiO_{2-x}N_x$/Beta-*x*% composite materials under visible light irradiation.

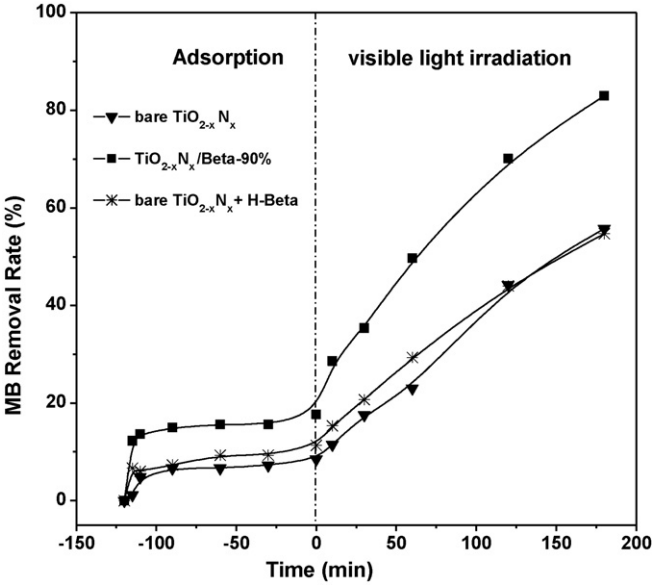

Fig. 7. Comparison of removal efficiency of MB on the $TiO_{2-x}N_x$/Beta-90%, the $TiO_{2-x}N_x$ and the mixed catalyst of bare $TiO_{2-x}N_x$ (90%) with H-Beta (10%) under visible light irradiation.

cially in the $TiO_{2-x}N_x$/Beta-10% sample. This further proves that titania particles were immobilized on the Beta zeolite by chemical bonds, which was in good accordance with the XPS results.

3.2. The photocatalytic activities

3.2.1. Effect of H-Beta zeolite support on the composite photocatalytic ability

To investigate the photocatalytic activities of the composite samples, the MB photodegradation under the visible light irradiation was carried out and compared with the bare $TiO_{2-x}N_x$ sample (shown in Fig. 6). In the adsorption–desorption process (from −120 to 0 min), it can be seen that for the parent H-Beta zeolite, the final methylene blue removal rate by adsorption could only reach 61%. With the increase of the TiO_2 loading, the amount of adsorbed MB by the composite materials was greatly reduced, and yet still higher than that of the bare N-doped TiO_2 sample. At the adsorption–desorption equilibrium point, the MB removal rates were 17%, 44% and 50% over the $TiO_{2-x}N_x$/Beta-90%, $TiO_{2-x}N_x$/Beta-40%, $TiO_{2-x}N_x$/Beta-10% catalysts, respectively, while the bare N-doped TiO_2 sample only achieved 8%. The addition of Beta zeolite appeared to enhance the composite adsorption ability, of which the order was also consistent with the BET results. However, the blockage in the pore channels on H-Beta support after TiO_2 addition may deteriorate with the increase of the TiO_2 loading.

After adsorption–desorption equilibrium, photodegradation of MB by parent H-Beta zeolite was performed under visible light irradiation as a blank experiment. In Fig. 6, no conversion can be seen by the parent H-Beta zeolite under the visible light irradiation. This means that the H-Beta zeolite was inert for the photodegradation of MB and any direct photocatalysis of MB was negligible. For the composite catalysts, after the photocatalytic reaction commencing, the MB concentration continued to decrease (from 0 to 180 min). The final MB removal achieved is 85%, 83%, 80% for the $TiO_{2-x}N_x$/Beta-90%, $TiO_{2-x}N_x$/Beta-40% and $TiO_{2-x}N_x$/Beta-10% catalysts, respectively. For the bare N-doped TiO_2 catalyst, the ultimate MB removal was only about 55%. It is evident that photocatalytic activities were greatly improved after adding the zeolite support compared to the bare N-doped TiO_2.

In order to demonstrate the synergistic role of the Beta zeolite support for photocatalytic activities in the composite samples more distinctively, the comparison of photocatalytic activity over the $TiO_{2-x}N_x$/Beta-90%, the bare N-doped TiO_2 sample and a mixture of bare N-doped TiO_2 (90%) with H-Beta (10%) was carried out. The results are shown in Fig. 7. For the loose mixture of naked N-doped TiO_2 with H-Beta, it was apparent that the MB removal by adsorption was higher than for the N-doped TiO_2 because of the addition of the Beta zeolite. However, the ultimate MB conversion (54.4%) after photocatalytic degradation was almost same lose to that of the bare N-doped TiO_2 (55.8%), and much lower than for the $TiO_{2-x}N_x$/Beta-90% (85.0%). This suggested that due to the successful loading of the titania on the Beta zeolite carrier, a synergistic effect existed that the Beta zeolite, which possessed a high surface area, could easily absorb the MB pollutant and supply a highly concentrated MB environment for the nearby titania to proceed the photocatalytic reaction.

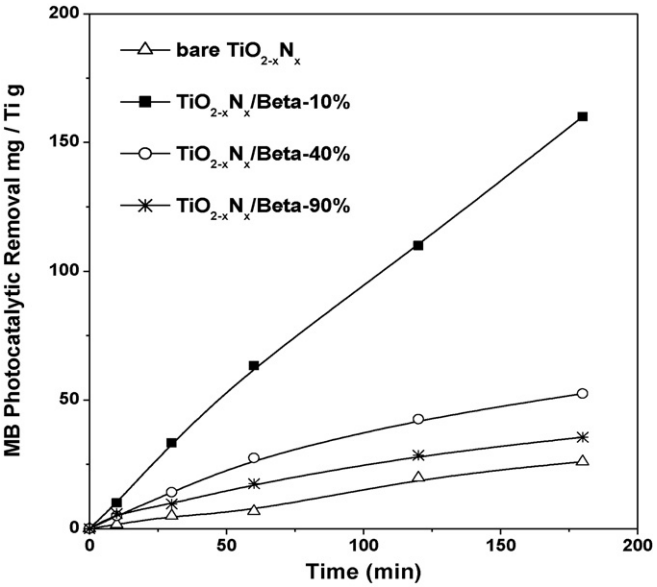

Fig. 8. Removal efficiency of MB on $TiO_{2-x}N_x$/Beta-*x*% catalysts under visible light irradiation.

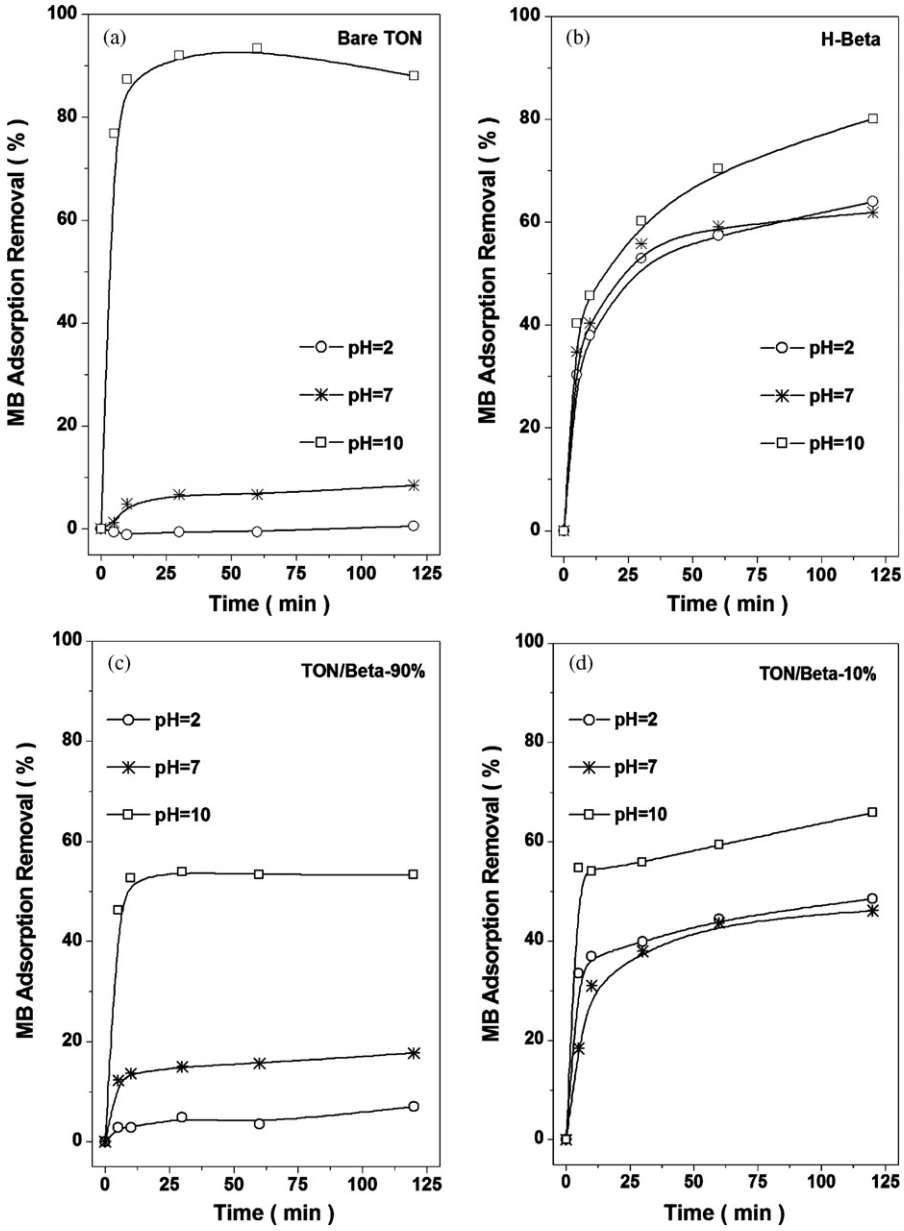

Fig. 9. Removal rate of MB on bare N-doped TiO_2 (a), H-Beta (b), $TiO_{2-x}N_x$/Beta-90% (c) and $TiO_{2-x}N_x$/Beta-10% (d) during adsorption process.

3.2.2. Determining optimal titania loading on the H-Beta zeolite support

One would expect that the titania loading on the H-Beta support affect the resulting photocatalytic ability of composites greatly. In Fig. 8, it is shown that for the bare $TiO_{2-x}N_x$ sample, the photocatalytic efficiency was the lowest compared with the $TiO_{2-x}N_x$/Beta composite samples. With the addition of H-Beta support, the photocatalytic efficiency was enhanced in the composite samples. For the $TiO_{2-x}N_x$/Beta-10% sample, extraordinarily high efficiency was obtained, which was 3–7 times higher than other samples. However, any higher titania loading than 10% appeared to have adverse effects. For the $TiO_{2-x}N_x$/Beta-90% sample, the photocatalytic efficiency was a little higher than the bare $TiO_{2-x}N_x$ sample. It is speculated that in composite samples some titania particles self-aggregate like the pure titania and the others link with the Beta support, while for the $TiO_{2-x}N_x$/Beta-10% sample, nano-sized titania particles were more well dispersed on the Beta support with strong bonding links. This could make the concentrated MB access the adjacent titania particles near the support more easily.

3.2.3. Influence of the solution pH values

In real applications, the pH value of wastewater varies depending on the source, which is an important factor influencing the photocatalytic activities [41]. Therefore, herein we investigated the effect of different pH values (pH = 2, pH = 7 and pH = 10) on the performance of composite samples.

Firstly, the adsorption of the bare $TiO_{2-x}N_x$ and H-Beta samples at different pH values were studied as references and the results are shown in Fig. 9(a) and (b). For the bare $TiO_{2-x}N_x$ sample, the adsorption ability was remarkably different at acidic and basic pH. The removal rate by adsorption could attain almost 90% at basic medium (pH = 10), while nearly no adsorption was observed at acidic medium (pH = 2). At the neutral pH, only a small removal rate (*ca.* 7%) could be achieved. Reportedly, the pH_{pzc} of titania is about 3.5–6.7, above which its surface became negatively charged. Since the MB is cationic dye, high pH medium would favour the MB adsorption apparently [41]. As for the H-Beta support, the similar trend of adsorption abilities was also found. Together, it is concluded that basic pH favoured the enhancement of the adsorp-

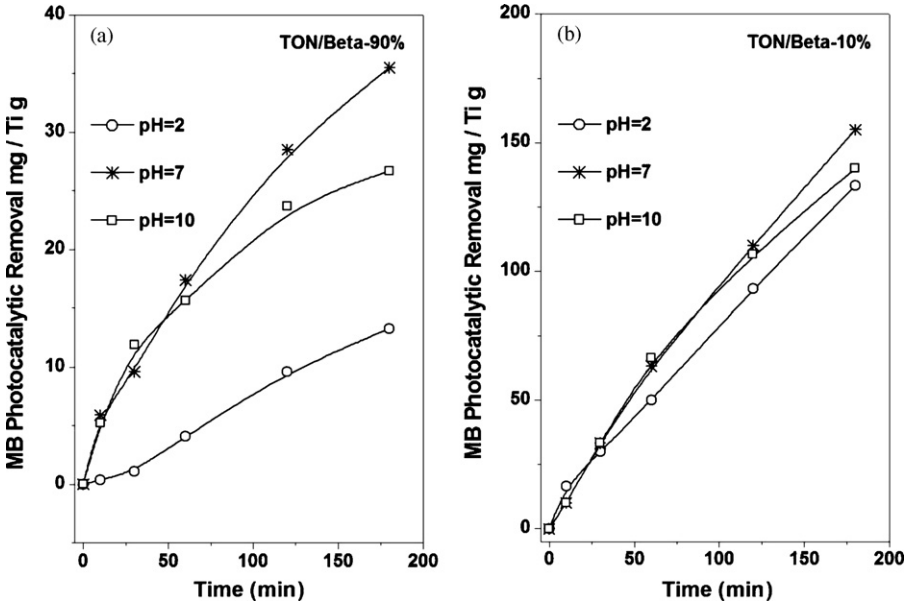

Fig. 10. Comparison of photocatalytic removal rate of MB on $TiO_{2-x}N_x$/Beta-90% (a) and $TiO_{2-x}N_x$/Beta-10% (b) samples under visible light irradiation.

tion ability both on the bare N-doped TiO_2 sample and on the H-Beta support, while this effect was more pronounced on the bare $TiO_{2-x}N_x$ sample than on parent H-Beta support. Fig. 9(c) and (d) shows the results about for MB adsorption of the $TiO_{2-x}N_x$/Beta-90% (a) and $TiO_{2-x}N_x$/Beta-10% (b) composite samples at different pH values. The MB adsorption behaviour of the $TiO_{2-x}N_x$/Beta-10% sample showed little difference to that of H-Beta. Both of them showed a great improvement of adsorption when the pH reached 10. For the $TiO_{2-x}N_x$/Beta-90% sample, the order of absorption between different pH values was similar to the bare $TiO_{2-x}N_x$ sample with slightly better adsorption ability at each pH due to the addition of small amount of H-Beta support.

In Fig. 10, further consideration has been given to the photocatalytic efficiency of the $TiO_{2-x}N_x$/Beta-90% and $TiO_{2-x}N_x$/Beta-10% composite samples for the MB degradation under different pH values. From Fig. 10(a), it can be seen that the photocatalytic efficiency of the $TiO_{2-x}N_x$/Beta-90% sample was influenced by the pH value greatly. As discussed before, the composite adsorption ability was associated with pH value strongly. Moderate adsorption (pH = 7) appears red to be optimal for the continuation of the photocatalytic reaction over the $TiO_{2-x}N_x$/Beta-90% sample. Higher basicity (pH = 10) with the overly strong MB adsorption could cover the titania active sites and thus hinder the absorption of light to progress the reaction. On the other hand, high acidity (pH = 2) with very weak or no adsorption was not beneficial to the reaction either, because of the low MB concentration adjacent to the active titania. The photocatalytic activity behaviour of the $TiO_{2-x}N_x$/Beta-10% sample was somewhat different, as seen in Fig. 10(b). Although the efficiency order was the same as that of $TiO_{2-x}N_x$/Beta-90% sample (pH = 7 > pH = 10 > pH = 2), the difference between the curves was narrow with a maximum point only at *ca.* 10%. Compared with $TiO_{2-x}N_x$/Beta-90% sample, $TiO_{2-x}N_x$/Beta-10% sample exhibited higher photocatalytic efficiency consistently at all three pH values.

4. Conclusions

A series of $TiO_{2-x}N_x$/Beta composite samples were prepared using a simple sol–gel method where nitrogen has been incorporated into the titania successfully. It is found that N-doped titania can be evenly dispersed on the Beta zeolite support at a low loading with chemical bonding between titania and the Beta zeolite support. It appeared that the synergistic absorption and photocatalysis of the $TiO_{2-x}N_x$/Beta composite materials could enhance the removal efficiency of methylene blue under visible light irradiation. All of the $TiO_{2-x}N_x$/Beta composite samples showed excellent photocatalytic activities under visible light irradiation, among which the $TiO_{2-x}N_x$/Beta-10% sample achieved the highest rate. This was potentially ascribed to the better dispersion of the $TiO_{2-x}N_x$ on support, which could make the concentrated MB access the adjacent titania particles on the zeolite support more easily. Further investigation also revealed that the $TiO_{2-x}N_x$/Beta-10% sample was consistent to be the most efficient composite material of the photocatalytic degradation of methylene blue in different pH solutions.

Acknowledgements

The authors acknowledge strategic research funding from University of South Australia. Thanks are also for the help in instrumental analysis conducted by Dr Andrew Michelmore at Mawson Institute, University of South Australia. The support from National Natural Science Foundation of China (20725723, 20703057) and National Basic Research Program of China (2004CB719500) are also appreciated.

References

[1] P.J. Senogles, J.A. Scott, G. Shaw, H. Stratton, Photocatalytic degradation of the cyanotoxin cylindrospermopsin, using titanium dioxide and UV irradiation, Water Res. 35 (2001) 1245–1255.
[2] L. Zou, B. Zhu, The synergistic effect of ozonation and photocatalysis on color removal from reused water, J. Photochem. Photobiol. A 196 (2008) 24–32.
[3] L. Lin, R.Y. Zheng, J.L. Xie, Y.X. Zhu, Y.C. Xie, Synthesis and characterization of phosphor and nitrogen co-doped titania, Appl. Catal. B: Environ. 76 (2007) 196–202.
[4] R.J. Tayade, R.G. Kulkarni, R.V. Jasra, Enhanced photocatalytic activity of TiO_2-coated NaY and HY zeolites for the degradation of methylene blue in water, Ind. Eng. Chem. Res. 46 (2007) 369–376.
[5] S.X. Liu, X.Y. Chen, Preparation and characterization of a novel activated carbon-supported N-doped visible light response photocatalyst ($TiO_{2-x}N_y$/AC), J. Chem. Technol. Biotechnol. 82 (2007) 453–459.
[6] Y.M. Xu, C.H. Langford, Photoactivity of titanium dioxide supported on MCM41, zeolite X, and zeolite Y, J. Phys. Chem. B 101 (1997) 3115–3121.
[7] K.F. Lin, P.P. Pescarmona, H. Vandepitte, D.D. Liang, G. Van Tendeloo, P.A. Jacobs, Synthesis and catalytic activity of Ti-MCM-41 nanoparticles with highly active titanium sites, J. Catal. 254 (2008) 64–70.
[8] J. Yang, J. Zhang, L.W. Zhu, S.Y. Chen, Y.M. Zhang, Y. Tang, Y.L. Zhu, Y.W. Li, Synthesis of nano titania particles embedded in mesoporous SBA-15:

characterization and photocatalytic activity, J. Hazard. Mater. 137 (2006) 952–958.
[9] T.P. Ang, C.S. Toh, Y.-F. Han, Characterization, and activity of visible-light-driven nitrogen-doped TiO_2–SiO_2 mixed oxide photocatalysts, J. Phys. Chem. C 113 (2009) 10560–10567.
[10] J.J. Xu, Y.H. Ao, D.G. Fu, C.W. Yuan, A synthesis of fluorine-doped titania-coated activated carbon under low temperature with high photocatalytic activity under visible light, J. Phys. Chem. Solids 69 (2008) 2366–2370.
[11] Y.J. Li, X.D. Li, J.W. Li, J. Yin, Photocatalytic degradation of methyl orange in a sparged tube reactor with TiO_2-coated activated carbon composites, Catal. Commun. 6 (2005) 650–655.
[12] Y. Tao, C.-Y. Wu, D.W. Mazyck, Removal of methanol from pulp and paper mills using combined activated carbon adsorption and photocatalytic regeneration, Chemosphere 65 (2006) 35–42.
[13] B. Zhu, L. Zou, Removal of color compounds from recycled water using combined activated carbon adsorption and AOP decomposition, J. Adv. Oxid. Technol. 12 (2009) 1–8.
[14] M.V. Shankar, S. Anandan, N. Venkatachalam, B. Arabindoo, V. Murugesan, Fine route for an efficient removal of 2,4-dichlorophenoxyacetic acid (2,4-D) by zeolite-supported TiO_2, Chemosphere 63 (2006) 1014–1021.
[15] M. Mahalakshmi, S.V. Priya, B. Arabindoo, M. Palanichamy, V. Murugesan, Photocatalytic degradation of aqueous propoxur solution using TiO_2 and H zeolite-supported TiO_2, J. Hazard. Mater. 161 (2009) 336–343.
[16] M. Takeuchi, T. Kimura, M. Hidaka, D. Rakhmawaty, M. Anpo, Photocatalytic oxidation of acetaldehyde with oxygen on TiO_2/ZSM-5 photocatalysts: effect of hydrophobicity of zeolites, J. Catal. 246 (2007) 235–240.
[17] A. Bhattacharyya, S. Kawi, M.B. Ray, Photocatalytic degradation of orange II by TiO_2 catalysts supported on adsorbents, Catal. Today 98 (2004) 431–439.
[18] D.I. Petkowicz, R. Brambilla, C. Radtke, C.D.S. da Silva, Z.N. da Rocha, S.B.C. Pergher, J.H.Z. dos Santos, Photodegradation of methylene blue by in situ generated titania supported on a NaA zeolite, Appl. Catal. A: Gen. 357 (2009) 125–134.
[19] M.V.P. Sharma, V. Durgakumari, M. Subrahmanyam, Solar photocatalytic degradation of isoproturon over TiO_2/H-MOR composite systems, J. Hazard. Mater. 160 (2008) 568–575.
[20] E.P. Reddy, L. Davydov, P. Smirniotis, TiO_2-loaded zeolites and mesoporous materials in the photocatalytic decomposition of aqueous organic pollutants: the role of the support, Appl. Catal. B: Environ. 42 (2003) 1–11.
[21] A.N. Ökte, Ö. Yılmaz, Characteristics of lanthanum loaded TiO_2-ZSM-5 photocatalysts: decolourization and degradation processes of methyl orange, Appl. Catal. A: Gen. 354 (2009) 132–142.
[22] A. Corma, H. Garcia, Zeolite-based photocatalysts, Chem. Commun. 9 (2004) 1443–1459.
[23] W. Zhang, L. Zou, L. Wang, Photocatalytic TiO_2/adsorbent nanocomposite prepared via wet chemical impregnation for wastewater treatment: a review, Appl. Catal. A: Gen. 71 (2009) 1–9.
[24] T.C. Jagadale, S.P. Takale, R.S. Sonawane, H.M. Joshi, S.I. Patil, B.B. Kale, S.B. Ogale, N-doped TiO_2 nanoparticle based visible light photocatalyst by modified peroxide sol–gel method, J. Phys. Chem. C 112 (2008) 14595–14602.
[25] J.F. Zhu, F. Chen, J.L. Zhang, H.J. Chen, M. Anpo, Fe^{3+}–TiO_2 photocatalysts prepared by combining sol–gel method with hydrothermal treatment and their characterization, J. Photochem. Photobiol. A 180 (2006) 196–204.
[26] A. Fuerte, M.D. Hernández-Alonso, A.J. Maira, A. Martínez-Arias, M. Fernández-García, J.C. Conesa, J. Soria, G. Munuera, Nanosize Ti–W mixed oxides: effect of doping level in the photocatalytic degradation of toluene using sunlight-type excitation, J. Catal. 212 (2002) 1–9.
[27] G.S. Wu, T. Nishikawa, B. Ohtani, A.C. Chen, Synthesis and characterization of carbon-doped TiO_2 nanostructures with enhanced visible light response, Chem. Mater. 19 (2007) 4530–4537.
[28] C. Burda, Y.B. Lou, X.B. Chen, A.C.S. Samia, J. Stout, J.L. Gole, Enhanced nitrogen doping in TiO_2 nanoparticles, Nano Lett. 3 (2003) 1049–1051.
[29] J.L. Gole, J.D. Stout, C. Burda, Y.B. Lou, X.B. Chen, Highly efficient formation of visible light tunable TiON photocatalysts and their transformation at the nanoscale, J. Phys. Chem. B 108 (2004) 1230–1240.
[30] Y.-M. Lin, Y.-H. Tseng, J.-H. Huang, C.C. Chao, C.-C. Chen, I. Wang, Photocatalytic activity for degradation of nitrogen oxides over visible light responsive titania-based photocatalysts, Environ. Sci. Technol. 40 (2006) 1616–1621.
[31] S.-K. Joung, T. Amemiya, M. Murabayashi, K. Itoh, Relation between photocatalytic activity and preparation conditions for nitrogen-doped visible light-driven TiO_2 photocatalysts, Appl. Catal. A: Gen. 312 (2006) 20–26.
[32] Y. Cong, J.L. Zhang, F. Chen, M. Anpo, Synthesis and characterization of nitrogen-doped TiO_2 nanophotocatalyst with high visible light activity, J. Phys. Chem. C 111 (2007) 6976–6982.
[33] X.B. Chen, Y.B. Lou, A.A.S. Samia, C. Burda, J.L. Gole, Formation of oxynitride as the photocatalytic enhancing site in nitrogen-doped titania nanocatalytsts: comparison to a commercial nanopowder, Adv. Funct. Mater. 15 (2005) 41–49.
[34] M. Alvaro, E. Carbonell, V. Formés, H. García, Enhanced photocatalytic activity of zeolite-encapsulated TiO_2 clusters by complexation with organic additives and N-doping, ChemPhysChem 7 (2005) 200–205.
[35] Z.-Y. Wang, F.-X. Zhang, Y.-L. Yang, B. Xue, J. Cui, N.-J. Guan, Facile postsynthesis of visible-light-sensitive titanium dioxide/mesoporous SBA-15, Chem. Mater. 19 (2007) 3286–3293.
[36] T.P. Ang, C.S. Toh, Y.-F. Han, Synthesis, characterization, and activity of visible-light-driven nitrogen-doped TiO_2–SiO_2 mixed oxide photocatalysts, J. Phys. Chem. C 113 (2009) 10560–10567.
[37] H.Q. Sun, Y. Bai, H.J. Liu, W.Q. Jin, N.P. Xu, G.J. Chen, B.Q. Xu, Mechanism of nitrogen-concentration dependence on pH value: experimental and theoretical studies on nitrogen-doped TiO_2, J. Phys. Chem. C 112 (2008) 13304–13309.
[38] T. Horikawa, M. Katoh, T. Tomida, Preparation and characterization of nitrogen-doped mesoporous titania with high specific surface area, Micropor. Mesopor. Mater. 110 (2008) 397–404.
[39] D.H. Sun, Y. Huang, B.X. Han, G.Y. Yang, Ti–Si mixed oxides prepared by polymer in situ sol–gel chemistry with the aid of CO_2, Langmuir 22 (2006) 4793–4798.
[40] X.F. Song, L. Gao, Synthesis, characterization, and optical properties of well-defined N-doped, hollow silica/titania hybrid microspheres, Langmuir 23 (2007) 11850–11856.
[41] A. Mills, M. Sheik, C. ÓRourke, M. McFarlane, Adsorption and photocatalysed destruction of cationic and anionic dyes on mesoporous titania films: reactions at the air–solid interface, Appl. Catal. B: Environ. 89 (2009) 189–195.